01 Jan 2018

A Constitutive Model for Entangled Polydisperse Linear Flexible Polymers with Entanglement Dynamics and a Configuration Dependent Friction Coefficient. Part I: Model Derivation

David W. Mead

Saman Monjezi

Joontaek Park
Missouri University of Science and Technology, parkjoon@mst.edu

Recommended Citation

D. W. Mead et al., "A Constitutive Model for Entangled Polydisperse Linear Flexible Polymers with Entanglement Dynamics and a Configuration Dependent Friction Coefficient. Part I: Model Derivation," *Journal of Rheology*, vol. 62, no. 1, pp. 121-134, American Institute of Physics (AIP), Jan 2018.
The definitive version is available at https://doi.org/10.1122/1.5009186

A constitutive model for entangled polydisperse linear flexible polymers with entanglement dynamics and a configuration dependent friction coefficient. Part I: Model derivation

Article *in* Journal of Rheology · January 2018
DOI: 10.1122/1.5009186

CITATION
1

READS
92

3 authors, including:

Saman Monjezi
Missouri University of Science and Technology
12 PUBLICATIONS **67** CITATIONS
SEE PROFILE

Joontaek Park
Missouri University of Science and Technology
33 PUBLICATIONS **100** CITATIONS
SEE PROFILE

A constitutive model for entangled polydisperse linear flexible polymers with entanglement dynamics and a configuration dependent friction coefficient. Part I: Model derivation

D. W. Mead[a)]

Mead Consulting, Bedford, New Hampshire 03110

S. Monjezi and J. Park[b)]

Chemical and Biochemical Engineering Department, Missouri University of Science and Technology, Rolla, Missouri 65409

(Received 7 April 2017; final revision received 3 August 2017; published 16 November 2017)

Abstract

A new polydisperse "toy" constitutive model is derived and developed from fundamental principles and ideas governing the nonlinear rheology of linear flexible polymers [Mead *et al*., J. Rheol. **59**, 335–363 (2015)]. Specifically, the new model is comprised of four fundamental pieces. First, the model contains a simple differential description of the entanglement dynamics of discrete entanglement pairs. Second, the model contains a differential description of the ij entanglement pair orientation tensor dynamics. Third, following a similar development by Mead and Mishler [J. Non-Newtonian Fluid Mech. **197**, 61–79 and 80–90 (2013).], a diluted stretch tube is constructed to describe the relative stretch of each component in the molecular weight distribution (MWD). Fourth, a description of configuration dependent friction coefficients is generated by generalizing the monodisperse formulation of Ianniruberto *et al*. [Macromolecules **45**, 8058–8066 (2012)]. The polydisperse stress calculator is developed from the orientation, stretch and entanglement density and is fundamentally different from other molecular models that assume a constant entanglement density. The resulting model is comprised of three differential evolution equations and is simple to code and fast to execute. The model can simulate arbitrary fast nonlinear flows of arbitrary MWD's. In the slow flow linear viscoelastic limit, the model collapses to the double reptation model. This welcome result has positive implications with respect to our model parameter determination [Ye *et al*., J. Rheol. **47**, 443–468 (2003); Ye and Sridhar, Macromolecules **38**, 3442–3449 (2005)] for making quantitative calculations. © *2017 The Society of Rheology*. https://doi.org/10.1122/1.5009186

I. INTRODUCTION

The linear rheology of linear [1], star [2], branched [3] and polydisperse blends [4] of entangled flexible polymers are all quantitatively understood at this point in time. Indeed entire research monographs have been written on this subject [5]. With respect to linear viscoelasticity, only the rheology of arbitrarily branched polymers remains to be quantitatively explained with tube models [6]. However, this relatively well understood state of affairs does not extend to the nonlinear molecular rheology of entangled flexible linear polymers. Since the linear viscoelastic material properties of mono and polydisperse linear polymer melts are well understood both theoretically and experimentally, it is only natural and logical that we now turn our attention to the molecular theory of the nonlinear viscoelastic material properties of polydisperse melts.

Although analytic molecular models of the nonlinear rheology of entangled polymers have been proposed previously [7–9], they all suffer from fundamental deficiencies that make them suspect. Given the importance of nonlinear rheology in any polymer processing operation understanding the rheology of flexible polymers at the molecular level is of fundamental importance both theoretically and practically. In addition to the practical relevance of our new model in the "forward" direction, we shall subsequently utilize nonlinear rheological measurements as a tool of analytic rheology by inverting the proposed nonlinear constitutive relationship to reveal the underlying molecular weight distribution (MWD) [5,10]. This feat has never been attempted let alone accomplished. To accomplish this feat we require a mathematically simple analytical model, as opposed to a stochastic simulator which may very well perform equally well in the forward direction, but is not invertible [11,12].

However, despite the importance of analytically constructed nonlinear molecular constitutive equations for flexible polymers even the fundamental principles underlying them have not been fully identified to date. For example, the two principal nonlinear analytic constitutive equations, the (Graham–Likhtman–McLeish–Milner) GLaMM [8] and (Mead–Larson–Doi) MLD models [7,9], both assume a *constant* entanglement density as reflected by the fact that the equilibrium plateau modulus scales the stress. In light of recent molecular dynamics simulations and theoretical studies, this fundamental assumption is almost certainly wrong. Specifically, the molecular dynamics simulations of

[a)]Electronic mail: meaddavid@hotmail.com
[b)]Author to whom correspondence should be addressed; electronic mail: parkjoon@mst.edu

Baig *et al.* [13] clearly demonstrate that the entanglement density of linear polyethylene melts decreases in fast nonlinear shear flows. Given the fundamental importance of the entanglement density in rheology getting a proper description of it is a theoretical imperative.

One of the fundamental principles underlying the formulation of general molecular constitutive equations of entangled polydisperse linear flexible polymers is the near universal adherence to the stress optical rule [14],

$$\mathbf{n}(t) = C\boldsymbol{\sigma}(t) + \textit{isotropic terms}. \tag{1}$$

Here, $\boldsymbol{n}(t)$ is the intrinsic birefringence and $\boldsymbol{\sigma}(t)$ is the deviatoric stress. The stress optical coefficient C is a scalar constant for a given entangled polymer melt/solution. The general validity of the stress optical rule in both linear *and* nonlinear flows of mono and polydisperse melts establishes that stress is proportional to the second moment of the segmental end-to-end vector, $\langle \mathbf{R}(t)\mathbf{R}(t)\rangle$, times a modulus, $G_N(t)$. A chain segment is the portion of chain trapped between successive entanglements along the chain. For monodisperse systems, the "toy" molecular model for entangled linear polymers can therefore be approximately written as [15,16]

$$\begin{aligned}\boldsymbol{\sigma}(t) &= \nu\langle \mathbf{RF}\rangle \approx \nu|\mathbf{R}|\langle F\rangle\langle \hat{R}\hat{R}\rangle \\ &\approx \underbrace{G_N(t)}_{\substack{\textit{Entanglement}\\ \textit{dynamics}}}\ \underbrace{k_s(t)\Lambda^2(t)}_{\substack{\textit{Stretch}\\ \textit{dynamics}}}\ \underbrace{\mathbf{S}_{tube}(t)}_{\substack{\textit{Orientation}\\ \textit{dynamics}}},\end{aligned} \tag{2}$$

where ν is the number density of chain segments and $\langle F\rangle = (kT/b)L^{-1}(x)$ is the average tension in the chain segment. Here, b is the length of a single Kuhn bond and $L^{-1}(x)$ is the inverse Langevin function. Note that we have invoked the tension-orientation decoupling approximation in Eq. (2) which is justified by the general validity of the stress optical rule. The stress optical rule will be violated whenever the nonlinear FENE spring factor k_s [see Eq. (20)] is significantly greater than unity, $k_s > 1$. This occurs when the fractional chain extension exceeds ~0.5 [18,19].

Although the above expression is for a monodisperse system the same principles will apply to each component in a polydisperse system. Thus, the three fundamental components of any molecular constitutive relationship are: (1) A quantitative description of the orientation dynamics, $\mathbf{S}_{tube}(t) = \langle \hat{R}\hat{R}\rangle$(orientation tensor which is defined as ensemble average of the unit end-to-end vector of a tube segment). (2) A quantitative description of the relative stretch dynamics, $\Lambda(t) = L(t)/L_{eq}(t)$ (the relative stretch of the "partially disentangled" chain which is defined as the ratio between the current tube contour length, $L(t)$, and the equilibrium length, $L_{eq}(t)$. (3) A quantitative description of the entanglement dynamics (ED) (which are manifested through the nonlinear time dependent modulus $G_N(t)$). These three essential constitutive equation components are, of course, all coupled and nonlinear. They also incorporate effects like a configuration dependent friction coefficient (CDFC) into the time scales of their descriptions.

The original Doi–Edwards model assumed no stretch and no ED (i.e., a constant modulus) only considering the orientation dynamics in Eq. (2). Consequently, the original family of Doi–Edwards tube and reptation models is restricted to the linear viscoelastic and weakly nonlinear flow regions. To access more general, strongly nonlinear fast flow situations, the Doi–Edwards model evolved naturally and systematically by next including the stretch dynamics to generate the (Doi–Edwards–Marrucci–Grizzuti) DEMG model [17–19]. The next step in the evolutionary progression of nonlinear molecular constitutive models was the MLD model which considered ED in the form of convective constraint release (CCR) in the restricted context of a constant net entanglement density [7,9]. The newly proposed (Mead–Park) MP model relaxes the final restriction of a constant entanglement density in order to access general fast nonlinear flow phenomena for polydisperse melts far from equilibrium. In the above manner, we can see the logical and systematic progression/evolution of molecular models starting from the seminal ideas proposed by de Gennes and Doi–Edwards [14]. [A genealogic tree for our model starting from the original Doi–Edwards model is presented in Appendix A (Fig. 6).] In this paper, we shall continue the natural evolution of molecular models by extending ideas of ED to polydisperse melts in general nonlinear flows.

In this paper, as in our previous work [15], we shall continue to use the term "tube" despite the fact that we believe that defining entanglements as discrete pairwise couplings (slip links) between two chains is a more accurate physical description of chain-chain uncrossability/confinement interactions [11,12]. Indeed, the traditional tube is an unhelpful concept in the nonlinear rheology of polydisperse systems. Invoking a mean field tube effectively fixes the entanglement density at a prescribed level consistent with the "tube diameter." Thus the tube concept is not conducive to simple descriptions of polydisperse pairwise ED since this would necessitate a continuously varying dynamic tube diameter. We believe that a simpler and more physical, natural approach is to describe the viscoelastic properties in terms of the pairwise ED as the conceptual paradigm rather than a mean field tube [20]. Hence, when we use the term tube in this paper we mean a series of discrete, oriented ij entanglement couplings along the chain. It is the orientation, stretch and survival dynamics of discrete ij entanglement pairs that provides the theoretical focus of the MP model of polydisperse linear polymers.

This paper is organized in the following manner: In Sec. II, we begin the development of the polydisperse MP model which has been in part previously published [15,21–23]. Section II A develops the partially disentangled and diluted stretch tube relative stretch relationship. Section II B derives the ij entanglement differential orientation tensor evolution equation. In Sec. II C, we generate the ij entanglement pair survival dynamical equation. Section II D takes up the issue of generating a general expression for CDFC. Sections II A–II D are concatenated in Sec. II E to develop the stress calculator in the partially disentangled tube. Finally, in Sec. III we summarize our model derivation and discuss the model properties. Because the polydispersity model is novel

in many ways we include a list of terms and their definitions in Nomenclature. Basic properties of the model, such as predicting shear modification, are presented in Paper II. Model parameter determination and validation of our model through simulation of model polydisperse system will be demonstrated in Paper III.

II. DERIVATION OF THE POLYDISPERSE MP TOY MODEL FOR ENTANGLED LINEAR FLEXIBLE POLYMERS

In our previous paper, we developed a toy constitutive model for entangled mono and polydisperse linear flexible polymers that displayed considerable promise in predicting both extensional and shear flow properties in the highly nonlinear flow regime [15,21]. In this paper, we continue our study of the constitutive model by detailing how to model polydisperse systems in arbitrary fast flows. We shall consider model MWDs with P discrete weight fractions, $\sum_{j=1}^{P} w_j = 1$. Here and throughout this paper subscripts denote discrete molecular weight components *not* tensor component indices unless stated explicitly otherwise.

As alluded to in the Introduction, we shall necessarily focus on the dynamics of discrete ij entanglement couplings where both i and j range from one to P. Indeed, as we proceed we shall see that our model is essentially an elaborate ij entanglement bookkeeping model where the orientation, stretch and survival dynamics are meticulously tracked for all P components in the MWD. With this overview in mind we proceed to develop the dynamics of each ij entanglement starting with the relative stretch dynamics in the partially disentangled and diluted stretch tube.

A. Derivation of the partially disentangled and diluted stretch tube relative stretch dynamics for an i-chain in an arbitrary MWD

As pointed out by Mishler and Mead [22,23], construction of a "naïve" polydispersity model is relatively straightforward given the monodisperse model developed in our previous publication (see Appendix B of [15]). However, this naïve construction does not take account of the fact that for systems with broad polydispersity lower molecular weight components may have an orientational relaxation time less than the stretch relaxation time of the high molecular weight component[1] (see Fig. 1). In this case, the low molecular weight components act effectively as "solvent" with respect to the stretch processes of the longer chains. This fact necessitates the construction of a "diluted stretch tube" to describe stretching processes for polymer systems with broad MWD's in nonlinear flows [22–24].

Before defining the diluted stretch tube we review the basic concepts and definitions concerning the "tube confinement" effect. The tube is a set of topological entanglements (slip links) that persist over a finite timescale. For example, for a timescale of infinity there are no slip link entanglements since the material is a liquid and can diffuse slowly throughout its environment. We shall define two distinct rheological time scales and construct their corresponding tubes. The first timescale we consider is τ_e, the equilibration time of a chain segment trapped between two discrete entanglements. Any topological entanglement that survives longer than τ_e is part of the set of entanglements defining this, the most basic tube. We call the set of topological entanglements surviving longer than τ_e the "Primary tube," which is in an equilibrium entanglement matrix. This tube shall serve as our reference tube which is necessary in order to define a known value of the plateau modulus, G_N^o, corresponding to a known entanglement density [see Fig. 2(A)]. The primary tube is the familiar tube we know from the linear viscoelastic rheology of mono and polydisperse linear and branched polymers. The primary tube is used in this regard to calculate stress in conventional linear viscoelastic (LVE) models since the equilibrium plateau modulus associated with this tube is known [1].

The next tube we construct is the "partially disentangled i-component tube" [see Fig. 2(B)]. The time scale associated with the entanglements comprising this tube is also τ_e, the same criterion used to construct the primary tube. The distinction between the primary tube and the partially disentangled i–tube is that, due to the nonlinear flow, a fraction of the entanglements comprising the primary tube have been shed. Hence the primary tube is disentangled by convection of entanglements off the tube ends at a rate sufficiently fast that the rate of creation of new entanglements by diffusive

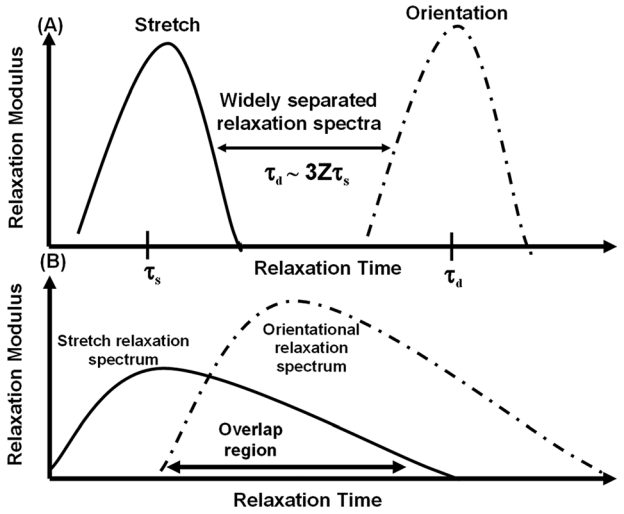

FIG. 1. Qualitative sketch of the orientational and stretch relaxation spectra for two hypothetical MWDs. Case (A) A narrow MWD ($(M_w/M_n) \lesssim 2$) where the stretch and orientational relaxation spectra are widely separated as envisioned in the original Doi–Edwards model. Case (B) A broad MWD ($(M_w/M_n) \gtrsim 2$) typical of most polydisperse commercial polymer systems where there is a wide *overlap* of the stretch and orientational relaxation spectra. Dispersion in the MWD and dispersion in the stretch and orientational relaxation spectra go hand in hand. Entanglement constraints that do not survive longer than the stretch relaxation time of the test chain do not impact the stretch dynamics of the high molecular weight components of a polydisperse system. This necessitates the construction of a diluted stretch tube to calculate the stretch of the high molecular weight components in broad MWD systems (see Fig. 2).

[1]We are temporarily ignoring the fact that the stretch relaxation time for blends is known to be affected by the stretch tube dilution [24] (see Appendix II and the following foot note).

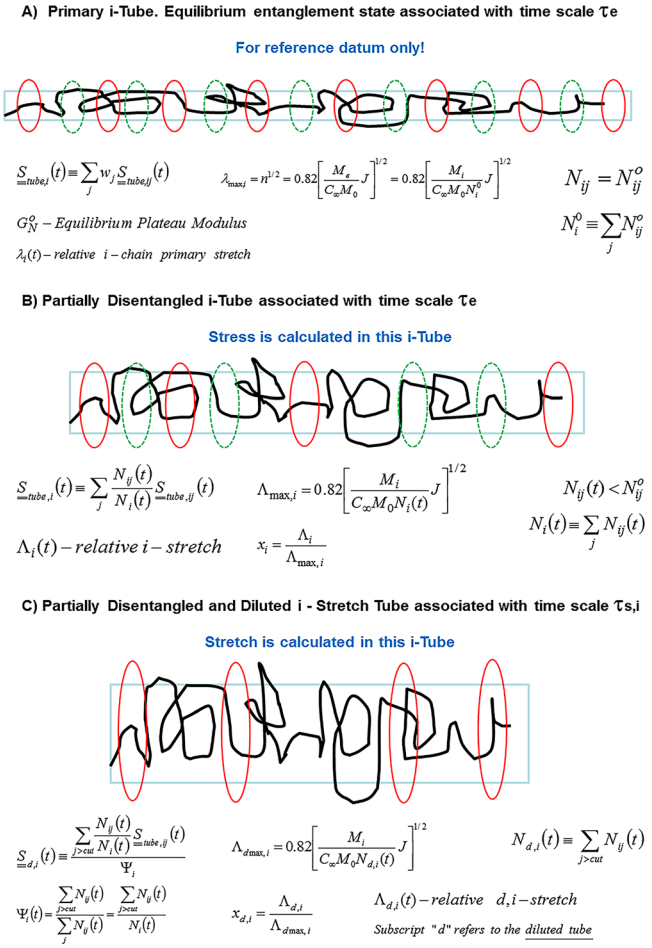

FIG. 2. Sketch of the hierarchy of three distinct unraveled tubes used in the calculation scheme for the polydisperse MP model. We use the term tube to refer to a set of discrete entanglement pairs and *not* a mean field tube in the classical sense. The construction of these ij entanglement pair tubes is motivated by the need to calculate the i-chain stretch in the presence of "solventlike" entanglements and entanglements lost by deformation (convection off the chain ends). The sketch illustrates a bidisperse system of fast relaxers (dotted links: green in online) and slow relaxers (solid links: red in online) relative to the stretch relaxation time of the red (i) chains. The partially disentangled tube (B) has fewer red *and* green entanglements. The partially disentangled and diluted stretch tube (C) has no green (fast) stretch entanglements. The primary tube (A) is the reference equilibrium entanglement state and is not directly used in MP calculations other than to define the plateau modulus, G_N^o. As in any polydispersity model, careful attention to the ij entanglement bookkeeping must be made. M_e is the equilibrium average entanglement molecular weight, M_i is the molecular weight of a polymer chain, M_0 is the monomer molecular weight, C_∞ is the characteristic ratio, n is the number of Kuhn bonds in an entanglement segment. J is the number of carbon-carbon sigma bonds in the backbone.

processes could not keep up. These issues will be discussed in more detail in Sec. II C where we derive the ij ED equation. We shall be calculating the stress contributions of each component in the MWD in the partially disentangled tube associated with it.

The final tube we construct is based on conventional time scale arguments. The Diluted stretch tube is defined as a subset of the dynamical constraints from the primary tube. The dynamical constraints in the i-component diluted stretch tube are comprised of entanglements that survive longer than a specific time scale. The particular time scale we are concerned with in stretching processes is the Rouse (stretch)

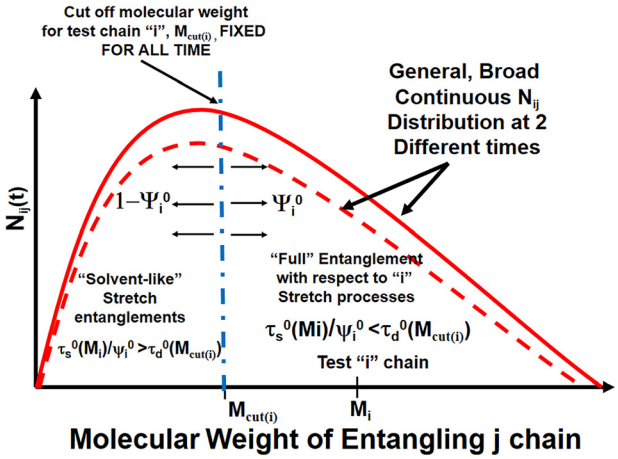

FIG. 3. Sketch of $N_{ij}(t)$ (number of j entanglements on a parent i-chain) for a typical broad MWD for a commercial polymer system with orientational and stretch relaxation spectra overlap. A given test chain of molecular weight, M_i, is chosen and the self-consistent cut-off criteria $(\tau^0_{s,i}(M_i))/(\Psi^0_i(M_i)\tau^0_{d,j}(M_{cut(i)})) = 1$ is applied which defines a conjugate molecular weight chain, $M_{cut(i)}$, that demarcates for all future calculations the boundary between solventlike chains with respect to stretch processes of the i chain and "full" entanglements with respect to i chain stretch processes. Note the similarity with Fig. 3 of Mishler and Mead [23]. Entanglement fractions replace weight fractions in the general MP model with variable, deformation dependent, entanglement densities, $N_{ij}(t)$. For an equilibrium entanglement density, $N^0_{ij} = w_j N^0_i$ and the two figures are effectively identical. The conjugate molecular weight $M_{cut(i)}$ is fixed for all time however the ij-entanglement distributions $N_{ij}(t)$ are not fixed, they are dynamic which makes $\Psi_i(t)$ dynamic as well.

relaxation time of the i-chain, $\tau^0_{s,i}$ [see Fig. 2(C)]. Other j-chains in the MWD matrix that relax their orientation faster than the stretch time scale, $\tau^0_{d,j} < \tau^0_{s,i}$, appear effectively solventlike with respect to stretch processes of the i-chain ($\tau_{d,j}$ is a tube disengagement or reptative relaxation time of the j-component). Thus, the borderline case $\tau^0_{s,i} = \tau^0_{d,j}$ demarcates the MWD into two pieces which depend on both the i and the j MWD component indices (see Fig. 3). The piece with the higher molecular weight species constitutes the set of MWD components that act as full entanglements with respect to stretch of the i-chain (viable dynamic entanglement in the diluted stretch tube). We denote this fraction as $\Psi^0_i = \sum_{j>cut(i)} w_j$.[2] The other piece with the lower molecular weight species act effectively as solvent or diluent with respect to stretch of the i-chain. Thus, for every i-chain there is a conjugate j-chain index that demarcates the split in the entanglements with respect to stretch of the i-chain. Note that this split and j demarcation index will be different for every i-chain. Thus there will be P distinct diluted stretch tubes to consider when computing the relative stretch of every i-chain in the MWD. These features manifest themselves whenever there is overlap in the stretch and

[2]Now we consider the stretch tube dilution effect (neglected in the previous footnote for easier understanding). The effective stretch relaxation time is: $\tau^{eff}_{s,i} = \tau^0_{s,i}/\Psi^0_i$ (see Appendix B and [24]). Here, the index "0" denotes equilibrium properties of the denoted variables and $1 - \Psi^0_i$ is the equilibrium "dilution" level of solvent like entanglements with respect to stretch of the long chains defined by the cutoff criteria $\tau^0_{s,i}/\Psi^0_i\tau^0_{d,j} > 1$ (see Fig. 3).

orientational relaxation spectra (see Fig. 1) and are effectively a ubiquitous feature of polydisperse systems.

We have constructed a hierarchy of three slip-link entanglement "tubes" required to calculate the i-chain stretch in arbitrary fast flows with an arbitrary MWD, as schematically illustrated in Fig. 2. The main difference between our model and the model by Mishler and Mead [22,23] is that the diluted stretch tube is also partially disentangled. Our new model contains a description of the ED such that we need to count the fraction of viable ij stretch entanglements and *not* weight fractions of the MWD to define the diluted stretch tube. Consequently, the modulus in other partially disentangled and/or diluted tubes will be lower and is calculated quantitatively relative to G_N^o. For the Mishler–Mead diluted tube we have[3]

$$\Psi_i^0 = \frac{\sum_{j>cut(i)} N_{ij}^0}{N_i^0} = \sum_{j>cut(i)} w_j. \tag{3}$$

Here, N_{ij}^0 is the equilibrium number of j-entanglements on an i-chain and is related to the total number of entanglements per i-chain at equilibrium by $N_{ij}^0 = w_j N_i^0$ where w_j is the weight fraction of j-chains and N_i^0 is the equilibrium number of entanglements for an i-chain. The j demarcation index splits the MWD into two pieces based on their relaxation time relative to the stretch relaxation time of the test chain. As noted above, Eq. (3) is valid when there are no net ED. When ED are present we have to generalize Eq. (3) to account for varying numbers of ij entanglements

$$\Psi_i(t) = \frac{\sum_{j>cut(i)} N_{ij}(t)}{N_i(t)}. \tag{4}$$

The above expression for $\Psi_i(t)$ represents the fraction of viable stretch tube entanglements on an i-chain at time t. The number of j-entanglements on a parent i-chain at time t is $N_{ij}(t)$. The total number of entanglements per i-chain at time t is $N_i(t)$. Note the clear distinction with Eq. (3) for the Mishler–Mead diluted stretch tube formulation. For the equilibrium entanglement microstructure, the factor $N_{ij}(t)/N_i(t)$ is simply equal to the weight fraction, $w_j = N_{ij}^0/N_i^0$, and the Mishler and Mead expression for $\mathbf{S}_{tube,i}$ is recovered [see also Eq. (19)]. Hence the factor $N_{ij}(t)/N_i(t)$ is a correction to account for nonequilibrium entanglement microstructure in the partially disentangled tube. Physically, the factor $N_{ij}(t)/N_i(t)$ accounts for differing amounts of Kuhn bonds oriented per ij entanglement pair as the entanglement microstructure is modified. In particular, $N_{ij}(t)/N_i(t)$ represents the fraction of Kuhn bonds on an i-chain oriented by j-entanglements. Note that for a monodisperse system $N_{ij}(t)/N_i(t)$ is equal to unity hence this important factor never arose in our previous monodisperse model [15]. It is important to note why we chose a constant cutoff $M_{cut(i)}$. We tried a dynamic cutoff criteria, however, there were cases when $\Psi_i(t)$ of a chain component became very small, which resulted in numerical instabilities and a discontinuous time-evolution of stress curve. Based on our subsequent work (Paper II and Paper III), we determined that the assumption of the constant cutoff criteria does *not* present any problems. Further investigation of the cutoff criteria will be performed in the future.

We have generalized the definition of $\Psi_i(t)$ to describe the dynamic ij entanglement microstructure which was not considered explicitly in the work of Mishler and Mead who defined Ψ_i^0 in terms of weight fractions which are not dynamic. Similar modifications have to be made in the definition of the orientation of the i-component diluted stretch tube orientation, $\mathbf{S}_{d,i}(t)$, Eq. (5) below,

$$\mathbf{S}_{d,i}(t) \equiv \frac{\sum_{j>cut(i)} \frac{N_{ij}(t)}{N_i(t)} \mathbf{S}_{tube,ij}(t)}{\Psi_i(t)}. \tag{5}$$

Once again, entanglement fractions have replaced weight fractions in the definition of $\mathbf{S}_{d,i}(t)$. The physical motivation behind this is to capture the orientation dynamics of the Kuhn bonds captured within the partially disentangled and diluted stretch tube. Counting the oriented Kuhn bonds is the fundamental idea underlying Eq. (5).

The i chain partially disentangled and diluted stretch tube segmental stretch equation under a velocity gradient $\boldsymbol{\kappa}(t)$ [see Fig. 2(C)] is presented below [7,22,23]. The subscript "d" always refers to the partially disentangled and diluted stretch tube (except in τ_d),

$$\dot{\Lambda}_{d,i}(t) = \underbrace{(\boldsymbol{\kappa} : \mathbf{S}_{d,i})\Lambda_{d,i}}_{\substack{affine\ stretch \\ of\ viable \\ entanglements}} - \underbrace{k_{d,i}(t)\Psi_i(t)\left(\frac{\Lambda_{d,i}-1}{\tau_{s,i}(t)}\right)}_{chain\ retraction} - \underbrace{\frac{1}{2}\left(1-|\mathbf{S}_{d,i}|\right)(\Lambda_{d,i}-1)\dot{\Phi}_{d,i}}_{CCR\ tube\ shortening}, \tag{6}$$

we define

$$\alpha_{d,i}(t) \equiv \frac{\Lambda_{d\max,i}(t)}{\lambda_{\max,i}} = \left[\frac{N_i^0}{\sum_{j>cut(i)} N_{ij}(t)}\right]^{\frac{1}{2}} = \left[\frac{N_i^0}{N_{d,i}(t)}\right]^{\frac{1}{2}}. \tag{7}$$

Here, the index "max" represents the maximum stretch of the stretch variable denoted. The parameter $\lambda_{\max,i}$ represents

[3] In order to calculate $\Psi_i^0 = \sum_{j>cut(i)} N_{ij}(t)/N_i(t)$ an iterative procedure is required to determine the position of the MWD cutoff index j. For the first iteration we choose $\Psi_i^0 = 1$ and determine a new dilution level and cut-off molecular weight, $M_{cut(i)}$. The new value of Ψ_i^0 is then fed into the cut-off criteria, $\tau_{s,i}^0(M_i)/(\Psi_i^0(M_i)\tau_{d,j}^0(M_{cut(i)})) = 1$, and this iterative process is repeated until convergence is achieved and the j cut-off index for an i-chain is determined for all future times (Fig. 3). Note that the position of the j-cut-off index, $M_{cut(i)}$, does *not* change with each further time step and this procedure need only be done once.

the maximum relative stretch in the primary tube where the entanglement density is constant and known [15]. Note that stretch relaxation due to disentanglement [15,25], $\dot{\alpha}_{d,i}(t)/\alpha_{d,i}(t)$, is included in $\dot{\Phi}_{d,i}$ rather than as an independent term in Eq. (6) [see Eq. (8)]. The fractional rate of diluted stretch tube matrix relaxation, $\dot{\Phi}_{d,i}$, defined as

$$\dot{\Phi}_{d,i}(t)=\frac{\sum\limits_{j>cut(i)}\frac{N_{ij}(t)}{N_i(t)}\left[\boldsymbol{\kappa}:\mathbf{S}_{d,j}-\frac{\dot{\Lambda}_{d,j}(t)}{\Lambda_{d,j}}+\frac{\dot{\alpha}_{d,j}(t)}{\alpha_{d,j}}+\frac{1}{\Lambda_{d,j}^2(t)\tau_{d,j}^1(t)}\right]}{\Psi_i(t)} \tag{8}$$

and the non-Gaussian chain tension amplification factor is defined as [16]

$$k_{d,i}(t)\equiv\frac{\mathrm{L}^{-1}\left(\frac{\Lambda_{i,d}(t)}{\Lambda_{d\max,i}(t)}\right)}{3\frac{\Lambda_{d,i}(t)}{\Lambda_{d\max,i}(t)}}\approx\frac{\left(3\lambda_{\max,i}^2{\alpha_{d,i}}^2-{\Lambda_{d,i}}^2\right)/\left(\lambda_{\max,i}^2{\alpha_{d,i}}^2-{\Lambda_{d,i}}^2\right)}{\left(3\lambda_{\max,i}^2{\alpha_{d,i}}^2-1\right)/\left(\lambda_{\max,i}^2{\alpha_{d,i}}^2-1\right)}. \tag{9}$$

Here, $\tau_{d,i}^1(t)=\tau_{d,i}(t)\left(\sum_k N_{ik}(t)/N_i^0\right)$ is the disentanglement modified tube disengagement time generalized for polydispersity from Eq. (A5) of Mead *et al*. [15], which is affected by partial disentanglement with CDFC accounted for. The factor $\left(\sum_k N_{ik}(t)/N_i^0\right)$ represents the reduced time it takes to reptate/diffuse into a new tube as the system disentangles and there are fewer tube segments (slip-links). Of course, $\tau_{d,i}(t)$ is the equilibrium disengagement time modified by CDFC, hence the time dependence [see Eq. (18)].

Thus Eq. (6) is effectively a conventional toy model stretch equation for the i-component partially disentangled and diluted tube. Equation (6) contains familiar terms such as affine stretch, chain retraction and constraint release driven tube shortening. This set of equations defines the partially disentangled and diluted stretch tube and the dynamics of how it stretches in a flow field.

The above equation set describes how to calculate the stretch of each i-chain in the MWD in the partially disentangled and diluted stretch tube. However, when we come to calculate the stress we shall need to account for the contributions of *all* the surviving entanglements. This of course is the partially disentangled tube [Fig. 2(B)]. In order to accomplish this, we need to relate the stretch in the partially disentangled and diluted tube, $\Lambda_{d,i}(t)$, to the stretch in the partially disentangled tube, $\Lambda_i(t)$. This stretch coupling analysis is done in Appendix B by invoking the principle that the net Kuhn bond orientation in both tube descriptions must be equal. It turns out that there are two separate solutions to this problem which we detail in Appendix B. One solution is due to Auhl *et al*. [24]

$$\Lambda_i\left(\frac{\Lambda_{\max,i}}{3}\right)\mathrm{L}^{-1}\left(\frac{\Lambda_i}{\Lambda_{\max,i}}\right)=(1-\Psi_i)+\Psi_i\left[\Lambda_{d,i}\left(\frac{\Lambda_{d\max,i}}{3}\right)\mathrm{L}^{-1}\left(\frac{\Lambda_{d,i}}{\Lambda_{d\max,i}}\right)\right] \tag{10}$$

and the other to Mishler and Mead [22,23]

$$\Lambda_i\left(\frac{\Lambda_{\max,i}}{3}\right)\mathrm{L}^{-1}\left(\frac{\Lambda_i}{\Lambda_{\max,i}}\right)=(1-\Psi_i)\left[\Lambda_i\left(\frac{\Lambda_{\max,i}}{3}\right)\mathrm{L}^{-1}\left(\frac{\Lambda_i}{\Lambda_{\max,i}}\right)\frac{3x_{d,i}}{\mathrm{L}^{-1}(x_{d,i})}\right]+\Psi_i\left[\Lambda_{d,i}\left(\frac{\Lambda_{d\max,i}}{3}\right)\mathrm{L}^{-1}\left(\frac{\Lambda_{d,i}}{\Lambda_{d\max,i}}\right)\right], \tag{11}$$

where Λ_i is a stretch in the partially disentangled i-stretch tube [see Fig. 2(B)]. $\Lambda_{d,i}$ is a stretch calculated in the diluted *and* partially disentangled i-stretch tube and $x_{d,i}=\Lambda_{d,i}/\Lambda_{d\max,i}$ is a fractional stretch in that diluted stretch tube [see Fig. 2(C)]. A previous comparison of the results from Eqs. (10) and (11) [22,23] showed that the Mishler–Mead stretch coupling relation (11) performs better than that derived by Auhl *et al*. [24]. The distinction between the two stretch coupling relationships (10) and (11) is discussed in detail in Appendix B. Further studies on comparing Eqs. (10) and (11) will be presented in our future publication (Paper III).

Thus, description of the stretch in polydisperse systems essentially requires elaborate bookkeeping measures; counting discrete ij entanglement pairs on the chain when ED and stretch tube dilution are operational (see Fig. 2 for a qualitative illustration of the model, identification of variables and the hierarchy of discrete ij entanglement tubes). Tubes are sets/ensembles of discrete ij entanglement pairs as described in the Introduction.

B. Derivation of the ij entanglement pair orientation dynamics

The next equation we derive is the differential orientation tensor evolution equation for an ij entanglement coupling, $\mathbf{S}_{tube,ij}(t)$. We are specifically interested in a differential form of the orientation evolution equation (as opposed to the traditional Doi–Edwards integral formulation) for speed of calculation. The issue of computational speed will become significant when we subsequently turn our attention to inverting the MP model to determine molecular weights from nonlinear viscoelastic experimental data.

The discrete ij entanglement pair orientation tensor differential evolution equations for two separate cases are presented below. The two cases we consider are first, full j-stretch entanglements on the parent i-chain, and second for solventlike j-stretch entanglements on an i-chain. A more complete explanation of the two separate cases is presented after Eq. (14) below.

The orientation tensor $\mathbf{S}_{tube,ij}(t)$ for the slow relaxing stretch full entanglements ($j>cut(i)$) in a flow described by the velocity gradient $\boldsymbol{\kappa}(t)$ evolves as [9,15]

$$\hat{\mathbf{S}}_{tube,ij}(t)+2\left(\boldsymbol{\kappa}(t):\mathbf{S}_{tube,ij}(t)\right)\mathbf{S}_{tube,ij}+\left(\frac{1-S_{Kuhn}}{\tau_{d,ij}(t)}\right)\left(\mathbf{S}_{tube,ij}-\frac{1}{3}\boldsymbol{\delta}\right)=\mathbf{0}. \tag{12}$$

And the orientation tensor $\mathbf{S}_{tube,ij}(t)$ for the fast relaxing ij solventlike stretch entanglements ($j<cut(i)$) evolves as

$$\hat{\mathbf{S}}_{tube,ij}(t) + 2\big(\boldsymbol{\kappa}(t) : \mathbf{S}_{tube,ij}(t)\big)\mathbf{S}_{tube,ij} + \left(\frac{1 - S_{Kuhn}}{\tau_{d,ij}(t)}\right)\big(\mathbf{S}_{tube,ij} - \mathbf{I}_{ij}(t)\big) = \mathbf{0}, \quad (13)$$

where $\hat{\mathbf{S}}_{tube,ij}(t)$ is the upper convected time derivative[4] and the tension induced orientation tensor, $\mathbf{I}_{ij}(t)$, in the fast relaxing entanglements ($j < cut(t)$) is calculated from a Kuhn-Grün analysis and is defined as Eq. 12 in the work by Mishler and Mead [22,23]

$$\mathbf{I}_{ij}(t) \equiv \left(1 - \frac{3x_{d,i}(t)}{\mathrm{L}^{-1}\big(x_{d,i}(t)\big)}\right)\mathbf{S}_{d,i}(t) + \frac{3x_{d,i}(t)}{\mathrm{L}^{-1}\big(x_{d,i}(t)\big)}\frac{1}{3}\boldsymbol{\delta}. \quad (14)$$

Recall our convention that the first index refers to the parent chain and the second index to the entangling chain. Hence there is in general no i-j symmetry and we must calculate P^2 orientation tensors to specify the orientation of all chain segments in the discrete MWD. The term $\hat{\mathbf{S}}_{tube,ij}(t)$ represents the codeformational rate of change of the orientation of an ensemble of stretchable rods following the convection and deformation of the fluid particle. The second term in Eq. (12) subtracts off the rate of stretch of the ensemble of rods such that the Trace is always unity, as it must be for any properly defined orientation tensor.

The final term in Eq. (12) represents the rate of relaxation of the orientation which is assumed to be proportional to the departure of the system from equilibrium, $\mathbf{S}_{tube,ij} - (1/3)\boldsymbol{\delta}$. While we believe that this is a reasonable description of j-entanglements constituting the partially disentangled and diluted tube, we believe that for those entanglements that are considered solventlike with respect to stretch of the i-chain be treated somewhat differently (see Fig. 2). Specifically, we believe that these fast relaxers with respect to i-chain stretch partially adopt the orientation of the parent i-chain diluted stretch tube, $\mathbf{S}_{d,i}(t)$, upon their creation. Herein lies the origin of the term $\mathbf{I}_{ij}(t)$ in Eqs. (13) and (14). Rather than having a newly created entanglement be born with an isotropic orientation, $(1/3)\boldsymbol{\delta}$, we model the process as having the newly created fast relaxing entanglement be born with partial orientation of the parent i-chain stretch tube, $\mathbf{S}_{d,i}(t)$. The degree to which the orientation is transmitted to the new entanglements will depend on the chain tension through a conventional Kuhn-Grün analysis (e.g., [16]).

The orientational relaxation time used in Eqs. (12) and (13) has its roots in the MLD model and is expressed as [7,9]

$$\frac{1}{\tau_{d,ij}(t)} = \frac{1}{\Lambda_{d,i}^2(t)\tau_{d,i}^1(t)} + \exp(-(\Lambda_{d,i} - 1)) \times \left[\boldsymbol{\kappa} : \mathbf{S}_{tube,j} - \frac{\dot{\Lambda}_j(t)}{\Lambda_j} + \frac{\dot{\alpha}_{d,j}(t)}{\alpha_{d,j}} + \frac{1}{\Lambda_{d,j}^2(t)\tau_{d,j}^1(t)}\right]. \quad (15)$$

[4]The upper convected time derivative is defined as [13]: $\hat{\mathbf{S}}_{tube,ij}(t) \equiv ((D\mathbf{S}_{tube,ij}(t))/Dt) - (\nabla v)^T \cdot \mathbf{S}_{tube,ij} - \mathbf{S}_{tube,ij} \cdot (\nabla v)$.

Here, $\exp(-(\Lambda_{d,i} - 1))$ is the empirical version of the "switch function" which apportions constraint release driven relaxation between stretch and orientation [26].

C. Derivation of the ij entanglement pair survival dynamics

The partially disentangled tube ij entanglement density evolution equation has been previously presented in equation B1 of Mead *et al.* [15]. We briefly review the terms and their meaning below. The number of j-entanglements on a parent i-chain, $N_{ij}(t)$, evolves as

$$\dot{N}_{ij}(t) = \frac{N_{ij}^0 - N_{ij}(t)}{\tau_{d,i}^1(t)} - \beta\left[\boldsymbol{\kappa} : \mathbf{S}_{tube,i} - \frac{\dot{\Lambda}_i(t)}{\Lambda_i} + \frac{\dot{\alpha}_i(t)}{\alpha_i(t)}\right] \times N_{ij}(t) + \frac{N_{ij}^0 - N_{ij}(t)}{\tau_{d,j}^1(t)}. \quad (16)$$

The term $(N_{ij}^0 - N_{ij}(t))/\tau_{d,i}^1(t)$ represents a driving force, $N_{ij}^0 - N_{ij}(t)$, divided by a characteristic time scale, $\tau_{d,i}^1(t)$ for the i-chain. It follows that the term $(N_{ij}^0 - N_{ij}(t))/\tau_{d,i}^1(t)$ represents a crude expression for the rate at which new ij entanglements are created/destroyed by reptative diffusion of the i-chain. Similarly, the last term $(N_{ij}^0 - N_{ij}(t))/\tau_{d,j}^1(t)$ represents the rate which ij entanglements are destroyed/created by reptative diffusion of the j-chain.

The second term in Eq. (16) above can be explained in a manner similar to that invoked for the monodisperse case [15]. Specifically, the term in brackets represents a net convective velocity of the j-entanglements off the ends of the parent i-chain. The first term, $\boldsymbol{\kappa} : \mathbf{S}_{tube,i}$ represents the uncorrected affine convection velocity off the chain ends. The two terms following the affine convection term, $-(\dot{\Lambda}_i(t)/\Lambda_i(t)) + (\dot{\alpha}_i(t)/\alpha_i(t))$, represent corrections to the relative ij entanglement velocity due to chain stretch and chain disentanglement respectively. Note that both of these correction terms are transient effects and do not impact the steady state. Finally, the factor β is an entanglement destruction "efficiency factor" first introduced by Ianniruberto and Marrucci [27] and has a value of about 0.12. This dimensionless factor was introduced such that the stress-shear rate curve is monotonic as it must be for stable shear flow.

The relative i-chain j-entanglement velocity correction term $-(\dot{\Lambda}_i(t))/\Lambda_i$ can be simply understood. When there is stretch but no chain retraction the term $-(\dot{\Lambda}_i(t))/\Lambda_i$ exactly cancels $\boldsymbol{\kappa} : \mathbf{S}_{i,tube}$ since for affine deformation the relative i-chain j-entanglement velocity is zero [7].

The derivation of the i-chain disentanglement velocity, $\dot{\alpha}_i(t)/\alpha_i(t)$, is identical to that presented by Mead *et al.* (see pages 337–338 of [15]) and will not be repeated here. The term $\alpha_i(t)$ physically reflects the dimensionless degree of i-chain disentanglement as measured by the enhanced extensibility and is defined in Eq. (17) below

$$\alpha_i(t) \equiv \frac{\Lambda_{\max,i}(t)}{\lambda_{\max,i}} = \left[\frac{N_i^0}{\sum_j N_{ij}(t)}\right]^{\frac{1}{2}} = \left[\frac{N_i^0}{N_i(t)}\right]^{\frac{1}{2}}. \quad (17)$$

Hence, $\dot{\alpha}_i(t)$ can be determined either numerically or analytically from Eqs. (17) and (16).

D. Derivation of the CDFC for a polydisperse system

In this section, we present the formulation of CDFC for a general polydisperse system. The fundamental idea underlying CDFC was presented by Ianniruberto *et al*. and we retain and generalize it here [28]. The idea is to quantify the relative orientation of the i-test chain Kuhn segment to that of the matrix Kuhn segments. One way to accomplish this is to take the projection of the test Kuhn segment orientation onto the matrix Kuhn segment orientation, $\mathbf{S}_{Kuhn,i} : \sum_j w_j \mathbf{S}_{Kuhn,j}$. So, CDFC will be some function of the relative orientation, $f(\mathbf{S}_{Kuhn,i} : \sum_j w_j \mathbf{S}_{Kuhn,j})$. We specify the unknown function f by demanding that it collapse to the monodisperse case described by Ianniruberto *et al*. [28]. Hence, CDFC impacts equally both the stretch and orientational relaxation times [15] in Eqs. (6) and (15)

$$\begin{aligned}\frac{\varsigma(t)}{\varsigma_{eq}} &= \frac{\tau_{s,i}(t)}{\tau^0_{s,i}} = \frac{\tau_{d,i}(t)}{\tau^0_{d,i}} = f\left(\mathbf{S}_{Kuhn,i} : \sum_j w_j \mathbf{S}_{Kuhn,j}\right) \\ &= 0.02239\left[\sqrt{\mathbf{S}_{Kuhn,i} : \sum_j w_j \mathbf{S}_{Kuhn,j}}\right]^{-1.64} \\ &= 0.02239\left[\sqrt{x_i^2 \mathbf{S}_{tube,i} : \sum_j w_j x_j^2 \mathbf{S}_{tube,j}}\right]^{-1.64}, \\ &\text{if } \sqrt{\mathbf{S}_{Kuhn,i} : \sum_j w_j \mathbf{S}_{Kuhn,j}} > 0.1. \end{aligned} \tag{18}$$

Here, the parameters are empirical and are based on a correlation developed in [28].

E. Derivation of the stress calculator

The above sections describe how we calculate the orientation and stretch of ij entanglements. The general non-Gaussian stress is calculated in the partially disentangled tube [9,15] [see Fig. 2(B)].

$$\begin{aligned}\boldsymbol{\sigma}(t) = \sum_{i=1}^{P} w_i \boldsymbol{\sigma}_i(t) = 3\sum_i \underbrace{\left(w_i\left(\frac{\sum_k N_{ik}(t)}{N_i^o}\right)G_N^0\right)}_{i\ \ chain\ modulus} \\ \times k_{s,i}(t)\Lambda_i^2(t)\underbrace{\sum_j \frac{N_{ij}(t)}{N_i(t)}\mathbf{S}_{tube,ij}(t)}_{\mathbf{S}_{tube,i}}, \end{aligned} \tag{19}$$

where [8]

$$\begin{aligned} k_{s,i}(t) &\equiv \frac{\mathrm{L}^{-1}\left(\frac{\Lambda_i(t)}{\Lambda_{\max,i}(t)}\right)}{3\frac{\Lambda_i(t)}{\Lambda_{\max,i}(t)}} \\ &\approx \frac{\left(3\lambda^2_{\max,i}\alpha_i{}^2 - \Lambda_i{}^2\right)/\left(\lambda^2_{\max,i}\alpha_i{}^2 - \Lambda_i{}^2\right)}{\left(3\lambda^2_{\max,i}\alpha_i{}^2 - 1\right)/\left(\lambda^2_{\max,i}\alpha_i{}^2 - 1\right)} \end{aligned} \tag{20}$$

and $\alpha_i(t)$ is defined in Eq. (17) above.

Equation (19) requires some additional explanation. Starting with the expression for the Kuhn bonds contained in the i tube, $\mathbf{S}_{tube,i}$. Once again the factor $N_{ij}(t)/N_i(t)$ appears rather than a simple weight fraction w_j. We remind the reader that $N_{ij}(t)/N_i(t)$ represents the fraction of Kuhn bonds on an i-chain oriented by j-entanglements.

In a similar manner the i-chain modulus is corrected from its equilibrium entanglement microstructure reference value with a similarly motivated factor, $w_i((\sum_k N_{ik}(t))/N_i^0)G_N^0$. The term $(\sum_k N_{ik}(t))/N_i^0$ represents the fractional decrease in the net number of entanglements on an i-chain. Hence, we are calculating the modulus/tension in the partially disentangled tube [Fig. 2(B)] by referring to the plateau modulus G_N^0 in the primary tube [Fig. 2(A)]. This is the sole purpose of defining the primary tube in the equilibrium entanglement state, i.e., in order to calculate the modulus and hence the stress in the partially disentangled tube.

Finally, Eq. (20) represents the non-Gaussian stretch enhancement to the stress and $\alpha_i(t)$ represents the enhanced extensibility of the chain in the partially disentangled tube relative to the primary tube.

III. SUMMARY

Although the tube model has been an important part of the research effort on polymer rheology for decades until recently there has been no general theory for the nonlinear rheology of polydisperse linear melts. The MLD model was the first such attempt at the nonlinear rheology of polydisperse linear polymers but is very restrictive in that it assumes a constant entanglement density. In this paper we have retained the binary, pairwise description of the entanglement interaction of the MLD model and introduced ED such that the entanglement density varies with the flow. As we shall subsequently see in future papers, this one change leads to some profound new physical phenomena such as shear modification of linear polymers [29–33]. We also note that there is a polydisperse model based on the multimode molecular stress function and the interchain pressure [34], which adopts a different approach from our model. Comparison with that model is beyond the scope of this paper but may be considered in the future.

There is one other distinctive feature of the MP constitutive model to point out. Specifically, since the MP model does not have a constant entanglement density the chains can disentangle and unravel in fast flows leading to highly extended chain conformations [25] (see Fig. 4). Nothing akin to this occurs in constant entanglement density models such as the MLD and GLaMM model families. The parameter that crudely characterizes the growth of extended conformations of an i-chain is α_i which is defined in Eq. (17). Thus, even the simple toy level MP molecular constitutive equation can yield some detailed information on the entanglement microstructure that is unavailable with other well-known constitutive models. These issues are extremely important if the MP model is to be used to calculate flow induced crystallization effects in polyethylene and polypropylene [35,36].

Although the MP model equation set may superficially appear quite complex the physical model it represents is actually rather simple both physically and mathematically. Computationally,

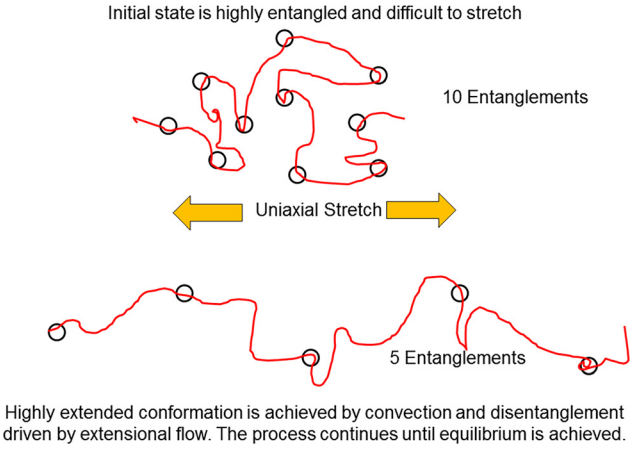

FIG. 4. Qualitative, two-dimensional illustration of the deformation driven generation of highly extended conformations. Flows with a high projection of the velocity gradient on the orientation, $\underline{\underline{\kappa}} : \underline{\underline{S}}$, are particularly effective at driving the disentangling process [see Eq. (16)]. When these convection processes overwhelm the diffusive re-entanglement processes disentanglement occurs resulting in a lower entanglement density and highly extended chain conformations. The MLD and GLaMM family of models *cannot* predict this type of highly extended conformation. It is believed that flow induced melt crystallization processes are severely impacted by the conformation and state of entanglement of the long chains [35,36].

we integrate the three first order ODE's, i.e., Eqs. (6), (12), and (16), using the midpoint method [37] (second order Runge-Kutta method) which is second order in the time step size, Δt (see Fig. 5). For very broad MWD systems, the fast relaxing entanglement pairs are integrated analytically using linear viscoelasticity analysis rather than severely decreasing the time step to capture their dynamics numerically. The speed and simplicity of the simulation software is important since we shall in the future invert the MP model to determine the MWD from nonlinear viscoelastic material functions such as transient extensional viscosity measurements. Application of our new model will be presented in Papers II, III and subsequent papers [38,39].

Finally, we comment on the conceptual similarity of the new MP model and pseudo network models introduced decades ago

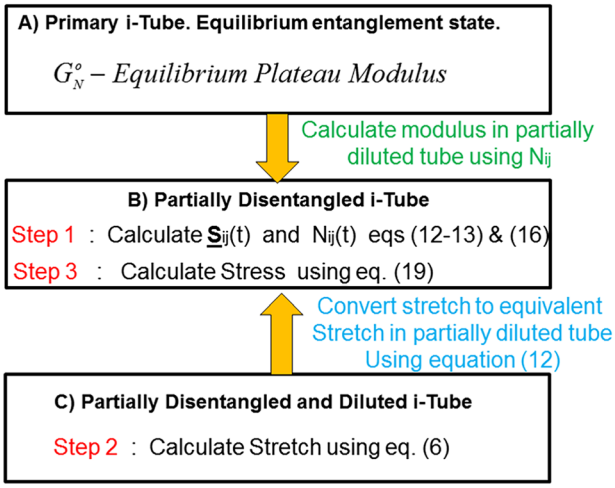

FIG. 5. Sketch of the numerical calculation scheme used at each discrete time step to calculate stress in polydisperse systems using the three tube hierarchy illustrated in Fig. 2. There are three initial value equations to be integrated at each discrete time step, Eqs. (12) and (13), (16) and (6). These are integrated using the midpoint method [37] in the order described above. The stress is calculated from Eq. (19) after the integrations at each time step are complete.

[40, p. 182]. The principal difference is that pseudo network models made no attempt to introduce molecularly based entanglement creation/destruction mechanisms. The MP model specifies the entanglement creation/destruction mechanisms and prescribes a molecular time scale for them although the ED equation (16) is still semiempirical. More detailed molecular descriptions at the tube coordinate level are planned to embellish the MP model.

Some comment on the number of MP model parameters and their determination is in order. It is easy to show that the MP model collapses to the "Double Reptation" model in the linear viscoelastic limit just as the polydisperse MLD model does. Consequently, we can use all the MLD model parameter determination literature [42,43] directly in the MP model to quantitatively determine the molecular parameters. The number of parameters required to perform quantitative calculations in the linear *and* nonlinear flow regimes for the MP toy model include the set of orientational and stretch relaxation times corresponding to each discrete slice of the MWD; $\{\tau_{d,i}^{(TM)}\}$ and $\{\tau_{s,i}^{(TM)}\}$[42,43]. The superscripts "TM" refer to "toy model." Additionally, we shall demonstrate in Paper III that in order to incorporate CLF into the model we shall have to consider *different* values of the plateau modulus for each slice of the discrete MWD, $\{G_{N,i}^{o(TM)}(M_i)\}$ [42,43].

ACKNOWLEDGMENTS

D.W.M. acknowledges the use of the computational facilities at the City College of New York. S.M. and J.P. acknowledge financial support from the Missouri University of Science and Technology.

NOMENCLATURE

The MP model develops a number of new ideas and concepts needed to describe polydispersity. In this section, we list all the terms and their definitions for quick reference (see Fig. 2).

$\Lambda_i(t)$	Relative stretch in the partially disentangled tube
$\Lambda_{d,i}(t)$	Relative stretch in the partially disentangled and diluted stretch tube
$\alpha_i(t) \equiv \frac{\Lambda_{\max,i}(t)}{\lambda_{\max,i}}$	Dimensionless ratio of the maximum relative stretches in the partially disentangled tube and the primary tube
$\alpha_{d,i}(t) \equiv \frac{\Lambda_{d\max,i}(t)}{\lambda_{\max,i}}$	Dimensionless ratio of the maximum relative stretches in the partially disentangled and diluted stretch tube and the primary tube
$\Psi_i(t) = \frac{\sum_{j>cut(i)} N_{ij}(t)}{N_i(t)}$	Fraction of all viable stretch tube entanglements on the i-th chain at time t (see Fig. 2)
$\mathbf{S}_{d,i}(t) \equiv \frac{\sum_{j>cut(i)} \frac{N_{ij}(t)}{N_i(t)} \mathbf{S}_{tube,ij}(t)}{\Psi_i(t)}$	Orientation of the partially disentangled and diluted stretch tube for the i-th chain
$\mathbf{S}_{tube,i} = \sum_j \frac{N_{ij}(t)}{N_i(t)} \mathbf{S}_{tube,ij}(t)$	Orientation of the partially disentangled tube for the i-th chain

$\mathbf{S}_{tube,ij}$ Orientation tensor for the ij entanglement pair

$\mathbf{S}_{Kuhn,i}$ Average orientation tensor for the Kuhn bonds on the i-th chain

$$k_{s,i}(t) \equiv \frac{\mathrm{L}^{-1}\left(\frac{\Lambda_i(t)}{\Lambda_{\max,i}(t)}\right)}{3\frac{\Lambda_i(t)}{\Lambda_{\max,i}(t)}} = \frac{\mathrm{L}^{-1}(x_i)}{3x_i}$$ Non-Gaussian stress amplification factor due to finite chain extensibility in the partially disentangled tube

$$k_{d,i}(t) \equiv \frac{\mathrm{L}^{-1}\left(\frac{\Lambda_{d,i}(t)}{\Lambda_{d\max,i}(t)}\right)}{3\frac{\Lambda_{d,i}(t)}{\Lambda_{d\max,i}(t)}} = \frac{\mathrm{L}^{-1}(x_{d,i})}{3x_{d,i}}$$ Non-Gaussian chain tension amplification factor due to finite chain extensibility in the partially disentangled and diluted tube

N_{ij}^0 The equilibrium number of j-entanglements on an i-chain

$N_{ij}(t)$ The dynamic number of j-entanglements on an i-chain

$N_i^0 \equiv \sum_j N_{ij}^0$ The total number of entanglements on the parent i-chain at equilibrium

$N_{d,i}(t) \equiv \sum_{j>cut(i)} N_{ij}(t)$ The total number of entanglements on the parent i-chain for the partially disentangled and diluted stretch tube. Also known as the "i-stretch tube" entanglements

$\dot{\Phi}_{d,i}(t)$ Fractional rate of destruction of partially disentangled and diluted stretch tube entanglements

$\tau_{d,i}^1(t)$ Tube disengagement time with the effects of partial disentanglement and CDFC accounted for

$\tau_{d,i}(t)$ Tube disengagement time in the equilibrium primary tube with the effects of CDFC accounted for

$\tau_{d,ij}(t)$ ij entanglement reptative relaxation time including the effects of CDFC

$\tau_{d,i}^0$ Bare equilibrium tube disengagement time without CDFC or entanglement effects

$\tau_{s,i}^0$ Bare stretch relaxation time without CDFC

$\tau_{s,i}(t)$ Stretch relaxation time including the effects of CDFC

β Entanglement destruction efficiency factor approximately equal to 0.12

$\boldsymbol{\kappa}$ Velocity gradient tensor

w_i Weight fraction of i-chains in a discrete MWD with P slices

G_N^0 Equilibrium plateau modulus defined in the primary tube

$\mathbf{S}_i^L = \langle \hat{r}_i \hat{r}_i \rangle$ Orientation due to the long-lived stretch entanglements only

$\mathbf{S}_{i,induced}$ Orientation induced in the short-lived stretch entanglements by the long-lived stretch entanglements. This quantity is determined by a Kuhn-Grün analysis.

APPENDIX A: GENEALOGICAL DIAGRAM FOR MP MODEL TRACING ITS ORIGINS FROM THE ORIGINAL DOI–EDWARDS MODEL

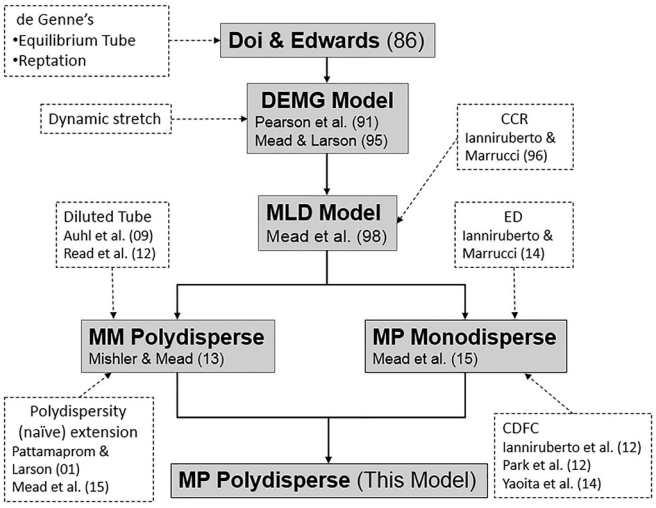

FIG. 6. Genealogical Diagram for MP model from Doi–Edwards Model: Gray boxes indicate the models. White boxes indicate the concepts used in each model. Note that the purpose of this chart is to demonstrate how and where our model was derived from not to display all the family models derived from Doi–Edwards, such as the GLaMM model [8].

APPENDIX B: DERIVATION AND COMPARISON OF THE STRETCH TUBE COUPLING RELATIONSHIPS; EQS. (10) AND (11)

In this Appendix, we analytically calculate the stretch tube coupling relationship, Eqs. (10) and (11) [22–24]. Since stretch is calculated in the partially disentangled and diluted tube [see Fig. 2(C)] and stress is calculated in the partially disentangled tube [Fig. 2(B)] a quantitative relationship between the stretch levels in each tube must be derived. Since in our model the diluent stretch entanglements do not participate in i-chain stretch processes, we are essentially calculating the induced stretch in these fast relaxing entanglements.[5] We shall demonstrate that although our model of

[5]Mishler and Mead [22,23] presented a physically similar two stretch tubes model. In this Appendix, we generalize the result of Mishler and Mead and demonstrate the relationship of that model to that of Auhl *et al*. [24].

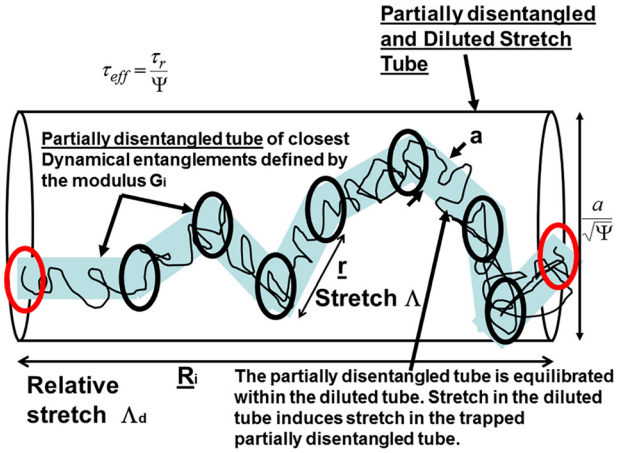

FIG. 7. Sketch of a solventlike entanglement with respect to stretch processes of the i-chain, trapped between two viable stretch entanglements. The fraction of viable stretch entanglements, "O's" at the both ends of the tube (red in online), is Ψ_i and that of solventlike entanglements with respect to stretch is $1-\Psi_i$. The orientation induced in the fast relaxing black entanglement "O" by stretch of the red viable stretch entanglements O's is determined by a Kuhn-Grün analysis.

the system is somewhat different from that of Auhl *et al.* [24], our general non-Gaussian result collapses identically to their stretch tube coupling relation for small extensions. Additionally, we derive the corresponding Mishler–Mead [22,23] tube coupling relationship and identify the specific differences and similarities with that of Auhl *et al.*

We begin with a sketch of the effective stretch entanglements on an i-chain and their noneffective, solventlike counterparts. Figure 7 illustrates an interior portion of an i-chain with long-lived discrete entanglements (red O's) and solventlike entanglements (black O's). This physical picture is consistent with our view the tube as a discrete set of entanglement pairs (slip links) rather than a mean field description.

The governing principle we invoke to determine the relationship between the two relative stretches in the nested tubes is that the stress associated with the long-lived entanglement pairs on an i-chain in either tube description must be the same, i.e., the net Kuhn bond orientation associated with the long-lived entanglement pairs contained in both tubes must be equal for both descriptions to be self-consistent. To implement this idea we must assign specific orientation levels in the partially disentangled tube due to the orientation and stretch of the long-lived diluted tube entanglements *only*.

The net partially disentangled tube orientation due only to the long-lived entanglements on an i-chain can be calculated approximately as the weighted sum of the oriented long-lived entanglements and the orientation induced in the short lived entanglements on the parent i-chain due solely to the long-lived entanglements

$$\begin{aligned}\mathbf{S}_i^L = \langle \hat{r}_i \hat{r}_i \rangle &\approx \underbrace{\Psi_i \mathbf{S}_{d,i}}_{\substack{\text{Long–lived}\\ \text{entanglements}}} + \underbrace{(1-\Psi_i)\mathbf{S}_{i,induced}}_{\substack{\text{Fast relaxing}\\ \text{entanglements}}} \\ &= \Psi_i \mathbf{S}_{d,i} + (1-\Psi_i)\left(1 - \frac{3x_{d,i}}{\mathrm{L}^{-1}(x_{d,i})}\right)\mathbf{S}_{d,i} \\ &\quad + (1-\Psi_i)\frac{3x_{d,i}}{\mathrm{L}^{-1}(x_{d,i})}\frac{1}{3}\boldsymbol{\delta}. \end{aligned} \tag{B1}$$

The induced orientation of the solventlike entanglements due to the stretch of the long-lived entanglements as defined by a Kuhn-Grün analysis [16], specifically (see Fig. 7) is

$$\begin{aligned}\mathbf{S}_{i,induced} &= \left(1 - \frac{3\frac{|\mathbf{R}|}{NL}}{L^{-1}\left(\frac{|\mathbf{R}|}{NL}\right)}\right)\hat{R}_i\hat{R}_i + \left(\frac{3\frac{|\mathbf{R}|}{NL}}{L^{-1}\left(\frac{|\mathbf{R}|}{NL}\right)}\right)\frac{1}{3}\boldsymbol{\delta} \\ &= \left(1 - \frac{3x_i}{L^{-1}(x_i)}\right)\mathbf{S}_{d,i} + \frac{3x_i}{L^{-1}(x_i)}\frac{1}{3}\boldsymbol{\delta}. \end{aligned} \tag{B2}$$

Here, $\hat{R}_i$ is the unit vector directed along the end-to-end vector $\mathbf{R}$ of an i-chain and $|\mathbf{R}|/NL = x_i$ is equivalent to the fractional extension.

In Eq. (B2) we are only considering orientation in the fast relaxing entanglement pairs on an i chain due directly to the long-lived entanglements. The orientation in these short-lived entanglement pairs due to subsequent deformation is described in Eqs. (12) and (13) and is not included in Eqs. (B1) and (B2). This deformation driven orientation is due to the dynamics of the short-lived entanglement pairs themselves and is not a direct consequence of the stretch of the long-lived entanglement pairs and hence is not included.

We note that the trace of $\mathbf{S}_i^L$ is unity as required for all properly formulated orientation tensors. Equation (B1) can be readily understood by recalling that the long-lived entanglements that reside in both the primary and diluted tubes are identical. The long-lived entanglements comprise a fraction Ψ_i of the partially diluted tube entanglements. The remaining fraction $1-\Psi_i$ of short-lived entanglements on the i chain have an induced orientation imparted during the re-entanglement process due to stretch of the long-lived entanglements [see Eqs. (12) and (13)].

The i-component stress due to the long-lived entanglement pairs *only* in the partially disentangled tube [Fig. 2(B)] is therefore

$$\boldsymbol{\sigma}_{i,L} = G_i\Lambda_i\left(\frac{\Lambda_{\max,i}}{3}\right)\mathrm{L}^{-1}\left(\frac{\Lambda_i}{\Lambda_{\max,i}}\right)\underbrace{\left[\left[\Psi_i + (1-\Psi_i)\left(1 - \frac{3x_{d,i}}{\mathrm{L}^{-1}(x_{d,i})}\right)\right]\mathbf{S}_{d,i} + (1-\Psi_i)\frac{3x_{d,i}}{\mathrm{L}^{-1}(x_{d,i})}\frac{1}{3}\boldsymbol{\delta}\right]}_{\text{orientation tensor in partially disentangled tube}}. \tag{B3}$$

We have effectively used Eq. (5) which introduces the dilution factor Ψ_i into the expression for the orientation of the diluted tube segments, i.e., $\Psi_i(t)\mathbf{S}_{d,i}(t) = \sum_{j>cut}\left(N_{ij}(t)/N_i(t)\right)\mathbf{S}_{tube,ij}(t)$. Recall that "solventlike" entanglements on the i-chain are similar to solvent only with respect to stretch relaxation processes of the i-chain and are absolutely not solventlike when stress is calculated for the partially disentangled tube in Eq. (B3). The factor G_i is the i-chain modulus in the partially disentangled tube, $G_i = ((\sum_k N_{ik}(t))/Ni_0)G_N^0$ [from Eq. (19)].

The corresponding i-component stress calculated in the partially disentangled and diluted stretch tube [Fig. 2(C)] yields

$$\boldsymbol{\sigma}_{d,i} = \underbrace{(\Psi_i G_i)}_{\substack{Modulus\\ in\ diluted\\ tube}}\left[\Lambda_{d,i}\left(\frac{\Lambda_{d\max,d}}{3}\right)\mathrm{L}^{-1}\left(\frac{\Lambda_{d,i}}{\Lambda_{d\max,i}}\right)\right]\underbrace{\mathbf{S}_{d,i}}_{\substack{orientation\\ tensor}} + \underbrace{G_i(1-\Psi_i)\frac{1}{3}\boldsymbol{\delta}}_{\substack{isotropic\\ "pressure"\\ term}}. \tag{B4}$$

In the low deformation limit matching (B3) and (B4) yields $G_i(1/3)\boldsymbol{\delta}$ for both equations. We demand that the arbitrary isotropic pressure term added in Eq. (B4) be a *constant* such that the isotropic terms match *only* in equilibrium, i.e., $P_{eq}\boldsymbol{\delta} = G_i(1/3)\boldsymbol{\delta}$. This is how we assign the isotropic term in Eq. (B4), i.e., so that the nominally arbitrary pressure matches in both stress descriptions for low orientations. The origins of the specific isotropic term in Eq. (B4) lie in the fact that we are comparing two separate Kramers analyses which result in differing numbers of segments cutting the plane. These points are discussed by Mishler and Mead [22,23].

Equating the two separate descriptions of i-component stress due to the long-lived entanglements only, Eqs. (B3) and (B4), yields

$$\begin{aligned}&\Lambda_i\left(\frac{\Lambda_{\max,i}}{3}\right)\mathrm{L}^{-1}\left(\frac{\Lambda_i}{\Lambda_{\max,i}}\right)\left[\left[\Psi_i + (1-\Psi_i)\left(1-\frac{3x_{d,i}}{L^{-1}(x_{d,i})}\right)\right]\right.\\ &\left.\times\mathbf{S}_{d,i} + (1-\Psi_i)\frac{3x_{d,i}}{\mathrm{L}^{-1}(x_{d,i})}\frac{1}{3}\boldsymbol{\delta}\right]\\ &= (1-\Psi_i)\frac{1}{3}\boldsymbol{\delta} + \Psi_i\left[\Lambda_{d,i}\left(\frac{\Lambda_{d\max,i}}{3}\right)\mathrm{L}^{-1}\left(\frac{\Lambda_{d,i}}{\Lambda_{d\max,i}}\right)\right]\mathbf{S}_{d,i}.\end{aligned} \tag{B5}$$

Equation (B5) is formulated by stipulating that the stress generated due *only* to the long-lived entanglement pairs be equal in each entanglement tube description. The notion that stress is held by discrete entanglement pairs that capture the test i-chain is the basis of the MP model [see Eq. (19)] and many other slip-link based models [11,12].

We can generate the general relationship between Λ_i and $\Lambda_{d,i}$ by taking the Trace of Eq. (B5). Since all properly formulated orientation tensors have a trace of unity we immediately see that

$$\begin{aligned}&\Lambda_i\left(\frac{\Lambda_{\max,i}}{3}\right)\mathrm{L}^{-1}\left(\frac{\Lambda_i}{\Lambda_{\max,i}}\right)\\ &= (1-\Psi_i) + \Psi_i\left[\Lambda_{d,i}\left(\frac{\Lambda_{d\max,i}}{3}\right)\mathrm{L}^{-1}\left(\frac{\Lambda_{d,i}}{\Lambda_{d\max,i}}\right)\right].\end{aligned} \tag{B6}$$

Equation (B6) defines the partially disentangled tube relative stretch of an i-chain, Λ_i, as a complex nonlinear function, $\Lambda_i = f_{stretch}(\Lambda_{d,i}, \Psi_i, \Lambda_{\max,i}, \Lambda_{d\max,i})$, which can be approximately and accurately calculated numerically in a simple manner (see Appendix C). Analysis of Eq. (B6) reveals that for low fractional extension levels $\Lambda_{d,i}/\Lambda_{d\max,i} \ll 1$,

$$\Lambda_i^2 = (1-\Psi_i) + \Psi_i\Lambda_{d,i}^2. \tag{B7}$$

Thus, the above Gaussian relationship between Λ_i, $\Lambda_{d,i}$, and Ψ_i derived by Auhl *et al.* [24] by an entirely different self-consistent Kuhn bond statistics method is retrieved in Eq. (B7) in the small fractional extension limit of Eq. (B6) [24 see Eq. (5)]. Hence, although Auhl *et al.* invoked a different model and analysis we arrive at the same result *if* we do not demand that the isotropic pressures be equal for *all* stretch levels.

Additionally, because the previous analysis generalizes that of Auhl *et al.* we also retrieve the same ancillary results derived by Auhl *et al.* In particular, we deduce that for small stretch levels near unity the effective stretch relaxation time in the diluted tube is related to the longest Rouse relaxation time of the chain by

$$\tau_{s,i}^{eff} = \frac{\tau_{s,i}}{\Psi_i}. \tag{B8}$$

Importantly, Eq. (B8) is observed experimentally for binary melts when the two components are widely separated in molecular weights [24].

Finally, for relative stretch levels near unity equation (B7) predicts that

$$\Lambda_i = 1 + \Psi_i(\Lambda_{d,i} - 1). \tag{B9}$$

Thus, stretch in the undiluted tube is significantly muted at low stretch levels relative to stretch of the diluted tube.

However, if we demand that the isotropic term in Eqs. (B3) and (B4) be equal for *all* stretch levels we generate a different result from that described above [22,23]. In this case, Eq. (B4) for the stress in the diluted tube [Fig. 2(C)] becomes

$$\boldsymbol{\sigma}_{i,diluted} = \underbrace{(\Psi_i G_i)}_{\substack{Modulus\\ in\ diluted\\ tube}} \left[\Lambda_{d,i}\left(\frac{\Lambda_{d\max,i}}{3}\right)\mathrm{L}^{-1}\left(\frac{\Lambda_{d,i}}{\Lambda_{d\max,i}}\right)\right] \underbrace{\mathbf{S}_{d,i}}_{\substack{orientation\\ tensor}} + \underbrace{G_i\Lambda_i\left(\frac{\Lambda_{\max,i}}{3}\right)\mathrm{L}^{-1}\left(\frac{\Lambda_i}{\Lambda_{\max,i}}\right)\frac{3x_{d,i}}{\mathrm{L}^{-1}(x_{d,i})}(1-\Psi_i)\frac{1}{3}\boldsymbol{\delta}}_{\substack{isotropic\\ "pressure"\\ term}}. \tag{B10}$$

The isotropic factor $G_i\Lambda_i\left(\Lambda_{\max,i}/3\right)\mathrm{L}^{-1}\left(\Lambda_i/\Lambda_{\max,i}\right)\left(3x_{d,i}/\mathrm{L}^{-1}(x_{d,i})\right)(1-\Psi_i)\frac{1}{3}\boldsymbol{\delta}$ in Eq. (B10) is generated such that Eqs. (B3) and (B9) match identically, i.e., they yield the same deviatoric *and* isotropic stress (pressure) for *all* stretch levels. Repeating the above analysis and equating Eqs. (B9) and (B3) and taking the trace yields the generalized (for non-Gaussian chains) result of Mishler and Mead [22,23]

$$\begin{aligned}\Lambda_i\left(\frac{\Lambda_{\max,i}}{3}\right)\mathrm{L}^{-1}\left(\frac{\Lambda_i}{\Lambda_{\max,i}}\right) &= (1-\Psi_i)\left[\Lambda_i\left(\frac{\Lambda_{\max,i}}{3}\right)\mathrm{L}^{-1}\left(\frac{\Lambda_i}{\Lambda_{\max,i}}\right)\frac{3x_{d,i}}{\mathrm{L}^{-1}(x_{d,i})}\right]\\ &\quad+\Psi_i\left[\Lambda_{d,i}\left(\frac{\Lambda_{d\max,i}}{3}\right)\mathrm{L}^{-1}\left(\frac{\Lambda_{d,i}}{\Lambda_{d\max,i}}\right)\right].\end{aligned} \tag{B11}$$

In the low stretch Gaussian limit (B11) reduces exactly to the result previously reported by Mishler and Mead

$$\Lambda_i = \Lambda_{d,i}. \tag{B12}$$

This contrasts starkly with the small stretch prediction of Auhl *et al*., Eq. (B9). We find that for systems with general polydisperse MWD's the Mishler–Mead stretch tube coupling relation yields *vastly* better predictions of the observed rheological behavior than does the Auhl *et al*. formulation [24]. The principal reason for the vastly better predictions is that the Mishler–Mead model does *not* suppress stretch at low stretch levels for the diluted stretch tube. Consequently, in this work we employ the Mishler–Mead formulation throughout [22,23].

APPENDIX C: DERIVATION OF AN APPROXIMATE ANALYTIC SOLUTION FOR Λ_i AS A FUNCTION OF $\Lambda_{d,i}$, Ψ_i, $\Lambda_{\max,i}$ AND $\Lambda_{d\max,i}$ FOR THE MP MODEL USING THE MISHLER–MEAD STRETCH TUBE COUPLING RELATION Eqs. (10) AND (11)

In this Appendix, we derive an approximate analytical solution to Mishler–Mead stretch tube coupling equation (B11) for Λ_i in terms of $\Lambda_{d,i}$, Ψ_i, $\Lambda_{\max,i}$ and $\Lambda_{d\max,i}$. Since stress is always calculated in the partially disentangled tube and stretch is calculated in the partially disentangled and diluted stretch tube an explicit analytic expression for Λ_i as a function of $\Lambda_{d,i}$ is very useful for numerical calculations. To realize this goal we will make use of the Padé approximant for the inverse Langevin function [41]. The Padé approximant for the inverse Langevin function of the fractional extension $\lambda_i/\lambda_{\max}$ is

$$\mathrm{L}^{-1}\left(\frac{\lambda_i}{\lambda_{\max}}\right) \approx \left(\frac{\lambda_i}{\lambda_{\max}}\right)\left[\frac{3-\left(\frac{\lambda_i}{\lambda_{\max}}\right)^2}{1-\left(\frac{\lambda_i}{\lambda_{\max}}\right)^2}\right]. \tag{C1}$$

Substituting Eq. (C1) into the inverse Langevin functions in Eq. (B6) and simplifying yields

$$\begin{aligned}&\left(\frac{\Lambda_i}{\Lambda_{\max,i}}\right)^2\left[\frac{3-\left(\frac{\Lambda_i}{\Lambda_{\max,i}}\right)^2}{1-\left(\frac{\Lambda_i}{\Lambda_{\max,i}}\right)^2}\right]\\ &\quad=\frac{\Psi_i\left[\Lambda_{d,i}\left(\frac{\Lambda_{d\max,i}}{3}\right)\mathrm{L}^{-1}\left(\frac{\Lambda_{d,i}}{\Lambda_{\max,id}}\right)\right]}{\left(\frac{\Lambda^2{}_{\max,i}}{3}\right)\left(1-(1-\Psi_i)\frac{3x_{d,i}}{\mathrm{L}^{-1}(x_{d,i})}\right)}\\ &\quad\equiv f(\Lambda_{d,i},\ \Psi_i, \Lambda_{\max,i}, \Lambda_{d\max,i}).\end{aligned} \tag{C2}$$

Since all stretch calculations are performed in the partially disentangled and diluted tube, hence the quantity $f(\Lambda_{d,i},\ \Psi_i, \Lambda_{\max,i}, \Lambda_{d\max,i})$ is known. If we define $y \equiv (\Lambda_i/\Lambda_{\max,i})$ then Eq. (C2) can be rearranged into a quadratic equation in y^2 with the function $f(\Lambda_{d,i},\ \Psi_i, \Lambda_{\max,i}, \Lambda_{d\max,i})$ as a known quantity defining the coefficients. Rearranging and solving explicitly for y^2 yields

$$y^2 = \frac{(3+f)-\sqrt{(3+f)^2-4f}}{2}. \tag{C3}$$

Note that only the solution to Eq. (C2) with a minus sign before the discriminant is physically meaningful. In this manner Λ_i can be expressed as a simple function of $\Lambda_{d,i}$, Ψ_i, $\Lambda_{\max,i}$ and $\Lambda_{d\max,i}$. We use the above approximate solution to the Mishler–Mead stretch tube coupling relation throughout this work.

The veracity of the above analysis turns on the accuracy of the Padé approximation for the inverse Langevin function. However, it has been established that the expression (C1) is an accurate approximation for the inverse Langevin function although other more mathematically complex formulations have also been presented by Cohen [41].

References

[1] Likhtman, A. E., and T. C. McLeish, "Quantitative theory for linear dynamics of linear entangled polymers," Macromolecules **35**, 6332–6343 (2002).

[2] Pearson, D. S., and E. Helfand, "Viscoelastic properties of star-shaped polymers," Macromolecules **17**, 888–895 (1984).

[3] McLeish, T. C. B., and R. G. Larson, "Molecular constitutive equations for a class of branched polymers: The pom-pom polymer," J. Rheol. **42**, 81–110 (1998).
[4] Pattamaprom, C., and R. G. Larson, "Predicting the linear viscoelastic properties of monodisperse and polydisperse polystyrenes and polyethylenes," Rheol. Acta **40**, 516–532 (2001).
[5] Dealy, J. M., and R. G. Larson, *Structure and Rheology of Molten Polymers* (Hanser, Munich, 2006), pp. 30–39.
[6] Desai, P. S., B.-G. Kang, M. Katzarova, R. Hall, Q. Huang, S. Lee, M. Shivokhin, T. Chang, D. C. Venerus, J. Mays, J. D. Schieber, and R. G. Larson, "Challenging tube and slip-link models: Predicting the linear rheology of blends of well-characterized star and linear 1,4polybutadienes," Macromolecules **49**, 4964−4977 (2016).
[7] Mead, D., R. Larson, and M. Doi, "A molecular theory for fast flows of entangled polymers," Macromolecules **31**, 7895–7914 (1998).
[8] Graham, R. S., A. E. Likhtman, T. C. McLeish, and S. T. Milner, "Microscopic theory of linear, entangled polymer chains under rapid deformation including chain stretch and convective constraint release," J. Rheol. **47**, 1171–1200 (2003).
[9] Mead, D., "Development of the 'binary interaction' theory for entangled polydisperse linear polymers," Rheol. Acta **46**, 369–395 (2007).
[10] Mead, D., "Determination of molecular weight distributions of linear flexible polymers from linear viscoelastic material functions," J. Rheol. **38**, 1797–1827 (1994).
[11] Andreev, M., R. N. Khaliullin, R. J. Steenbakkers, and J. D. Schieber, "Approximations of the discrete slip-link model and their effect on nonlinear rheology predictions," J. Rheol. **57**, 535–557 (2013).
[12] Schieber, J. D., and M. Andreev, "Entangled polymer dynamics in equilibrium and flow modeled through slip links," Annu. Rev. Chem. Biomol. Eng. **5**, 367–381 (2014).
[13] Baig, C., V. G. Mavrantzas, and M. Kroüger, "Flow effects on melt structure and entanglement network of linear polymers: Results from a nonequilibrium molecular dynamics simulation study of a polyethylene melt in steady shear," Macromolecules **43**, 6886–6902 (2010).
[14] Doi, M., and S. F. Edwards, *The Theory of Polymer Dynamics* (Oxford University, Oxford, 1986).
[15] Mead, D. W., N. Banerjee, and J. Park, "A constitutive model for entangled polymers incorporating binary entanglement pair dynamics and a configuration dependent friction coefficient," J. Rheol. **59**, 335–363 (2015).
[16] Larson, R. G., *Constitutive Equations for Polymer Melts and Solutions: Butterworths Series in Chemical Engineering* (Butterworth-Heinemann, Oxford, 2013).
[17] Pearson, D., E. Herbolzheimer, N. Grizzuti, and G. Marrucci, "Transient behavior of entangled polymers at high shear rates," J. Polym. Sci., Part B: Polym. Phys. **29**, 1589–1597 (1991).
[18] Mead, D. W., and L. G. Leal, "The reptation model with segmental stretch I. Basic equations and general properties," Rheol. Acta **34**, 339–359 (1995).
[19] Mead, D. W., D. Yavich, and L. G. Leal, "The reptation model with segmental stretch II. Steady flow properties," Rheol. Acta **34**, 360–383 (1995).
[20] Everaers, R., S. K. Sukumaran, G. S. Grest, C. Svaneborg, A. Sivasubramanian, and K. Kremer, "Rheology and microscopic topology of entangled polymeric liquids," Science **303**, 823–826 (2004).
[21] Park, J., D. W. Mead, and M. M. Denn, "Stochastic simulation of entangled polymeric liquids in fast flows: Microstructure modification," J. Rheol. **56**, 1057–1081 (2012).
[22] Mishler, S., and D. W. Mead, "Application of the MLD 'toy' model to extensional flows of broadly polydisperse linear polymers: Part I–Model development," J. Non-Newtonian Fluid Mech. **197**, 61–79 (2013).
[23] Mishler, S., and D. W. Mead, "Application of the MLD 'toy' model to extensional flows of broadly polydisperse linear polymers: Part II. Comparison with experimental data," J. Non-Newtonian Fluid Mech. **197**, 80–90 (2013).
[24] Auhl, D., P. Chambon, T. C. McLeish, and D. J. Read, "Elongational flow of blends of long and short polymers: Effective stretch relaxation time," Phys. Rev. Lett. **103**, 136001 (2009).
[25] Desai, P. S., and R. G. Larson, "Constitutive model that shows extension thickening for entangled solutions and extension thinning for melts," J. Rheol. **58**, 255–279 (2014).
[26] Mead, D. W., "Derivation of the "switch function" in the Mead–Larson–Doi theory," Rheol. Acta **50**, 631–643 (2011).
[27] Ianniruberto, G., and G. Marrucci, "Convective constraint release revisited," J. Rheol. **58**, 89–102 (2014).
[28] Ianniruberto, G., A. Brasiello, and G. Marrucci, "Simulations of fast shear flows of PS oligomers confirm monomeric friction reduction in fast elongational flows of monodisperse PS melts as indicated by rheooptical data," Macromolecules **45**, 8058–8066 (2012).
[29] Breuer, G., and A. Schausberger, "Recovery of shear modification of polypropylene melts," Rheol. Acta **50**, 461–468 (2011).
[30] Heitmiller, R., R. Naar, and H. Zabusky, "Effect of homogeneity on viscosity in capillary extrusion of polyethylene," J. Appl. Polym. Sci. **8**, 873–880 (1964).
[31] Schreiber, H., A. Rudin, and E. Bagley, "Separation of elastic and viscous effects in polymer melt extrusion," J. Appl. Polym. Sci. **9**, 887–892 (1965).
[32] Teh, J., A. Rudin, and H. Schreiber, "Shear modification of a linear low density polyethylene," J. Appl. Polym. Sci. **30**, 1345–1357 (1985).
[33] Schertzer, R., A. Rudin, and H. P. Schreiber, "Shear and thermal history effects in polypropylene melts," J. Appl. Polym. Sci. **31**, 809–821 (1986).
[34] Narimissa, E., and M. H. Wagner, "A hierarchical multimode molecular stress function model for linear polymer melts in extensional flows," J. Rheol. **60**, 625–636 (2016).
[35] Yamazaki, S., F. Gu, K. Watanabe, K. Okada, A. Toda, and M. Hikosaka, "Two-step formation of entanglement from disentangled polymer melt detected by using nucleation rate," Polymer **47**, 6422–6428 (2006).
[36] Eder, G., H. Janeschitz-Kriegl, and S. Liedauer, "Crystallization processes in quiescent and moving polymer melts under heat transfer conditions," Prog. Polym. Sci. **15**, 629–714 (1990).
[37] Süli, E., and D. F. Mayers, *An Introduction to Numerical Analysis* (Cambridge University, Cambridge, 2003).
[38] Mead, D. W., S. Monjezi, and J. Park, "A constitutive model for entangled polydisperse linear flexible polymers with entanglement dynamics and a configuration dependent friction coefficient. Part II: Model derivation," J. Rheol. (unpublished).
[39] Mead, D. W., S. Monjezi, and J. Park, "A constitutive model for entangled polydisperse linear flexible polymers with entanglement dynamics and a configuration dependent friction coefficient. Part III: Comparison with experimental data," J. Rheol. (unpublished).
[40] Doi, M., *Soft Matter Physics* (Oxford University, Oxford, 2013).
[41] Cohen, A., "A Padé approximant to the inverse Langevin function," Rheol. Acta **30**, 270–273 (1991).
[42] Ye, X., R. G. Larson, C. Pattamaprom, and T. Sridhar, "Extensional properties of mono and bidisperse polystyrene solutions," J. Rheol. **47**, 443–468 (2003).
[43] Ye, X., and T. Sridhar, "Effects of the polydispersity on rheological properties of entangled polystyrene solutions," Macromolecules **38**, 3442–3449 (2005).